

**Discovery of a potent and selective covalent inhibitor and activity-based probe  
for the deubiquitylating enzyme UCHL1, with anti-fibrotic activity**

Nattawadee Panyain,<sup>†</sup> Aurélien Godinat,<sup>†</sup> Thomas Lanyon-Hogg,<sup>†</sup> Sofía Lachiondo-Ortega,<sup>†,‡</sup>  
Edward J. Will,<sup>†</sup> Christelle Soudy,<sup>‡</sup> Katie Mason,<sup>§</sup> Sarah Elkhalfa,<sup>§</sup> Lisa M. Smith,<sup>§</sup> Jeanine A.  
Harrigan,<sup>§</sup> and Edward W. Tate<sup>\*,†,‡</sup>

<sup>†</sup> Department of Chemistry, Molecular Sciences Research Hub, Imperial College London,  
London, W12 0BZ, UK

<sup>‡</sup> The Francis Crick Institute, London, NW1 1AT, UK

<sup>§</sup> Mission Therapeutics Ltd, Moneta, Babraham Research Campus, Cambridge, CB22 3AT,  
UK

\*Correspondence should be addressed to E.W.T. ([e.tate@imperial.ac.uk](mailto:e.tate@imperial.ac.uk)).

**ABSTRACT:** Ubiquitin carboxy-terminal hydrolase L1 (UCHL1) is a deubiquitylating enzyme which is proposed as a potential therapeutic target in neurodegeneration, cancer, and liver and lung fibrosis. Herein we report the discovery of the most potent and selective UCHL1 probe (IMP-1710) to date based on a covalent inhibitor scaffold and apply this probe to identify and quantify target proteins in intact human cells. IMP-1710 stereoselectively labels the catalytic cysteine of UCHL1 at low nanomolar concentration in cells, and we show that a previously claimed UCHL1 inhibitor (LDN-57444) fails to engage UCHL1 in cells. We further demonstrate that potent UCHL1 inhibitors block pro-fibrotic responses in a cellular model of idiopathic pulmonary fibrosis, supporting a potential therapeutic role for UCHL1 inhibition and providing a basis for future therapeutic development of selective UCHL1 inhibitors.

Targeting of the ubiquitin (Ub) proteasome system has emerged as a highly promising therapeutic strategy, and deubiquitylating enzymes (DUBs) have attracted increasing interest as drug targets.<sup>1</sup> To study DUB biology and inhibition, Ub-derived activity-based probes (ABPs) have been developed that covalently bind to DUB active sites allowing isolation or profiling in cell lysates.<sup>2</sup> However, Ub-based probes are non-selective between DUBs and membrane-impermeable, limiting their applications to lysates and highlighting the need for complementary small molecule ABPs to profile DUB activity in intact cells. We recently characterized a cell-permeable small molecule probe for ubiquitin-specific proteases (USPs), alongside an alkyne-tagged ABP analogue that enabled activity-based protein profiling (ABPP) of USP activity for the first time in intact cells.<sup>3</sup>

Ubiquitin Carboxy-Terminal Hydrolase L1 (UCHL1) belongs to the UCH protease family, which feature a characteristic Cys-His-Asp catalytic triad. Although UCHL1 has well-characterized DUB activity, some studies suggest UCHL1 may also function as a Ub ligase or mono-Ub stabilizer, and its biological functions are not yet fully understood.<sup>4</sup> UCHL1 is abundantly expressed in the brain where it is involved in apoptosis regulation, learning, and memory, whilst UCHL1 dysregulation is linked to diseases including neurodegeneration,<sup>4</sup> cancers<sup>5-6</sup> and fibrosis.<sup>7</sup>

A screening and hit optimization campaign by Mission Therapeutics identified a series of novel cyanamide-containing UCHL1 inhibitors.<sup>8</sup> Recognizing the potential of these inhibitors as covalent probes for UCHL1, we selected a potent inhibitor (**1**; example 27 in reference 8) and designed analogue IMP-1710 (**2**) bearing an alkyne tag strategically placed in line with established structure-activity relationships (Figure 1a, Figure S1).<sup>8</sup> The alkyne enables functionalization post-inhibition with 'capture' reagents *via* copper (I)-catalyzed azide-alkyne cycloaddition (CuAAC) for analysis.<sup>9-10</sup> We first examined biochemical UCHL1 inhibition in a fluorescence polarization (FP) assay using Ub-Lys-TAMRA.<sup>11</sup> Compound **2** showed improved

UCHL1 inhibition ( $IC_{50}$  38 nM, 95% CI 32-45 nM) over parent compound **1**, ( $IC_{50}$  90 nM, 95% CI 79-100 nM), following 30 min pre-incubation. However, the (*R*)-enantiomer of **1** (IMP-1711, **3**) was >1000-fold less active than **1**, demonstrating a highly stereoselective interaction with UCHL1 and providing a useful negative control (Figure S1). We further characterized inhibition kinetics by **1** and **2** through determination of  $k_{obs}/I$  (7400 (95% CI 5200-9700) 11000 (95% CI 7700-13000)  $M^{-1}s^{-1}$ , respectively, Figure. S2), and slow recovery of activity following dilution demonstrated these inhibitors are slowly reversible, in line with previous reports of this warhead class (Figure. S2).<sup>12</sup> Cross-screening against a panel of 20 DUBs demonstrated that compounds **1** and **2** exhibit exquisite selectivity for UCHL1 (Figure 1b), whereas control compound **3** was inactive against all tested DUBs (Figure S1). Cellular UCHL1 activity was demonstrated in breast cancer cells (Cal51) stably expressing FLAG-UCHL1 using a Ub-vinyl methyl ester probe (HA-Ub-VME) in a homogeneous time resolved fluorescence (HTRF) assay.<sup>13</sup> Compounds **1** and **2** effectively engaged UCHL1, with in-cell  $IC_{50}$  values of 820 and 110 nM, respectively (Figure S3). Concentration-dependent competition by **1** and **2** for selective UCHL1 HA-Ub-VME labeling was confirmed through immunoblot analysis (Figure 1c, S4). Potencies were in line with biochemical data, whilst compound **3** did not inhibit UCHL1 in cells, consistent with previous results (Figure S1).

We next compared our probes to the most potent literature UCHL1 inhibitor, isatin *O*-acyl oxime LDN-57444 (Figure 1a). LDN-57444 has been reported as a reversible, Ub-competitive UCHL1 inhibitor with  $IC_{50}$  880 nM against recombinant UCHL1,<sup>14</sup> and has been widely used as a tool inhibitor in UCHL1 studies in disease models.<sup>6-7, 15-16</sup> However, engagement of UCHL1 in intact cells has not previously been demonstrated. We profiled LDN-57444 in a range of assays, including biochemical activity and capacity to bind UCHL1 in intact cells (Figure S1, S3, S4), and were surprised to discover that LDN-57444 failed to engage UCHL1 in any assay ( $IC_{50}$  >300  $\mu$ M) or inhibit any DUBs tested (Table S1, Figure S1), effectively invalidating this compound as a DUB inhibitor.

Direct target engagement using **2** was examined in HEK293 cells treated with compound for 60 min, followed by lysis and ligation to azide-TAMRA-biotin capture reagent (AzTB, Figure S5) through CuAAC (Figure 2a).<sup>9</sup> In-gel fluorescence revealed a single major target at ~25 kDa, labeled in a concentration-dependent manner. Labeling appeared complete at 125 nM **2**, whilst concentrations >500 nM suggested some labeling of other proteins (Figure 2b). Labeling was confirmed by biotin pulldown and immunoblotting, with UCHL1 significantly enriched at 30 nM **2**, and maximal at 125 nM, with minimal or no detectable labeling of UCHL3, UCHL5 and DUBs from other families (Figure 2c, Figure S6). Time course experiments demonstrated maximal labeling within 60 min (Figure S7), and **2** remained stable in media for >72 h without loss of activity (Figure S8). Incubation of recombinant UCHL1

(5  $\mu$ M) with **1** or **2** (12.5  $\mu$ M) for 60 min led to single modification of UCHL1 by LC-ESI-MS (Figure 3a). Modification specifically at the UCHL1 catalytic cysteine (Cys90) was confirmed by tryptic digest and nanoLC-MS/MS (Figure S9, Supplementary Data S1). To confirm the catalytic Cys requirement for modification in intact cells, we overexpressed FLAG-tagged wild type (WT) UCHL1, or C90A or C90S mutants in HeLa cells, which lack endogenous UCHL1, and treated with **2**.<sup>17</sup> In-gel fluorescence and immunoblot analyses demonstrated that only WT UCHL1 is labeled by **2**, confirming dependence on UCHL1 catalytic activity for cellular target engagement (Figure 3b, Figure S10).<sup>17</sup> Taken together, these data demonstrate **2** is a bona fide UCHL1 ABP that rapidly targets endogenous UCHL1 in cells in a strictly activity-dependent manner.

To determine selectivity of **2** across the proteome, unbiased quantitative chemical proteomic profiling (Figure 2a) was employed in HEK293 cells treated with **2** (2, 20 or 200 nM) or vehicle (DMSO) control, for 10, 60 or 180 min. Cell lysates were ligated by CuAAC to azide-arginine-biotin (AzRB, Figure S5) capture reagent,<sup>9</sup> and labeled proteins enriched on dimethylated NeutrAvidin-agarose beads. Proteins were digested on-resin with LysC followed by trypsinization,<sup>18</sup> labeled with tandem mass tags (TMT) to enable relative quantification between conditions, and samples analyzed by nanoLC-MS/MS. UCHL1 was significantly enriched by **2** in a concentration-dependent manner, with marginal enrichment of UCHL3 at higher concentrations and no significant enrichment of any other DUB (Figure 2d, Figure S11); UCHL1 enrichment was similar at all time points, consistent with previous results (Figure S7). Only two proteins, UCHL1 and fibroblast growth factor receptor 2 (FGFR2), were significantly enriched at 20 nM ABP **2** treatment, with UCHL1 by far the major target (Figure S12, Supplementary Data 2). No significant change protein abundance was detected in whole proteome analysis following ABP **2** treatment (Figure S13, Supplementary data 3), suggesting that **2** does not substantially alter global protein homeostasis. In-gel fluorescence and immunoblot analysis further confirmed ABP **2** can profile activity of endogenous UCHL1 across different cell types, including endothelial cells (EA.hy926) and adenocarcinoma human alveolar basal epithelial cells (A549) with excellent selectivity (Figure S14).

To identify selective targets of parent compound **1** and differentiate between selective labeling and non-specific pulldown, competitive ABPP was performed.<sup>19-20</sup> HEK293 cells were treated with **1**, **3** or LDN-57444 for 1 h, followed by **2** (20 nM) for 10 min. Immunoblot analysis demonstrated dose-dependent UCHL1 labeling reduction with parent compound **1** at nanomolar concentrations, whereas no competition was observed with control compound **3** or LDN-57444, confirming **3** as an effective negative control and LDN-57444 as inactive against UCHL1 in cells (Figure 4a-b). In-cell proteome-wide competitive ABPP was performed by quantitative chemical proteomics, showing that across the whole proteome UCHL1

responds strongly to **1** in a concentration-dependent manner, but does not respond with inactive control **3** or LDN-57444 (Figure 4c, Figure S15, Supplementary Data 4). UCHL3 shows a small response to **1**, whilst outside the DUB family FGFR2 responds (Figure S15), suggesting these proteins are possible minor off-targets of **1**.

UCHL1 has recently been reported as an emerging therapeutic target in development of fibrosis.<sup>7, 21</sup> Pharmacological UCHL1 inhibition was therefore investigated in primary human lung cells derived from idiopathic pulmonary fibrosis (IPF) patients. Fibroblast-to-myofibroblast transition (FMT) was stimulated by transforming growth factor beta 1 (TGF- $\beta$ 1) using alpha-smooth muscle actin ( $\alpha$ SMA) as a disease-relevant marker for transition (Figure 5a).<sup>22-23</sup>  $\alpha$ SMA production was validated by high content imaging analysis (HCA) of three donor cell lines in response to TGF- $\beta$ 1 stimulation, alongside response to 1 h pre-treatment with TGF- $\beta$ 1 receptor kinase inhibitor SB525334 (1  $\mu$ M).<sup>24</sup> FMT was consistently induced by TGF- $\beta$ 1 and inhibited by SB525334 in all donor fibroblasts, with strong Spearman correlation between biological replicates (Figure S16). Donor cells were treated with compounds **1**, **2**, **3**, LDN-57444 or FDA-approved IPF drug nintedanib,<sup>25</sup> and response to TGF- $\beta$ 1 measured after 3 days by staining and HCA quantification of  $\alpha$ SMA and nuclei (DAPI). Compounds **1** and **2** (1  $\mu$ M) demonstrated >50% FMT inhibition (IC<sub>50</sub> 15 nM and 410 nM, respectively), with comparable potency to nintedanib (Figure 5b). Nuclear count was stable <5  $\mu$ M compound, providing a therapeutic window between inhibition and cytotoxicity (Figure S17). Compound **3** showed reduced  $\alpha$ SMA inhibition compared to **1** and **2**, with similar cytotoxicity to **2**. Although LDN-57444 showed evidence for weak  $\alpha$ SMA inhibition, this was concurrent with increased cytotoxicity over the same concentration range, suggesting that LDN-57444 toxicity drives decreased  $\alpha$ SMA (Figure S18).

In summary, we report discovery and characterization of the most potent and selective small-molecule DUB ABP (**2**) to date, enabling robust detection of UCHL1 activity in living cells at low nanomolar concentrations. The only previously reported UCHL1 ABP is >150-fold less potent than **2** and has multiple significant off-targets,<sup>12</sup> with no selectivity over UCHL3. UCHL1 labeling by **2** is strictly activity-dependent, occurring only at the catalytic cysteine, and providing a new chemical tool to examine UCHL1 activity in various intact cell types. ABPP demonstrated that parent compound **1** is a potent UCHL1 inhibitor that targets the active site cysteine residue with impressive selectivity in cells, and that UCHL1 inhibition is highly stereoselective providing an ideal control compound (**3**) for future studies. Further, evidence from multiple assays (biochemical, cellular, proteomics) demonstrates that, contrary to previous reports, LDN-57444 does not engage UCHL1, which invalidates this compound as a tool inhibitor and suggests that previously reported studies using LDN-57444 may be subject to reinterpretation.<sup>14, 26</sup> Finally, we show that **1** and **2**, but not the inactive enantiomer **3**, can

completely suppress fibrotic phenotypes in IPF cellular models without substantial cytotoxicity, highlighting the potential of UCHL1 inhibitors for treatment of fibrosis. **1** and **2** therefore represent powerful and selective probes to explore UCHL1 activity with potential application to substrate identification, mode of action studies, and cellular target profiling, which can accelerate future development of UCHL1 inhibitors as potential fibrosis therapeutics.

## **ASSOCIATED CONTENT**

### **Supporting Information**

The Supporting Information is available free of charge on the ACS Publications website at DOI: XXXXXXXX.

Additional results and materials and methods for protein production, biochemical assay, cell-based experiment, chemical proteomic sample preparation and data analysis, FMT assay. Detailed chemical synthesis for all synthesized compounds, <sup>1</sup>H, <sup>13</sup>C NMR spectra and HRMS data (PDF).

Datafiles of protein identification and quantification from the proteomic experiments (XLSX)

Supplementary Data S1: Peptide lists of compound-modified peptide identification

Supplementary Data S2: Protein lists of ABP **2** target engagement

Supplementary Data S3: Protein lists of whole proteome analysis

Supplementary Data S4: Protein lists of competitive ABPP

The mass spectrometry proteomics data have been deposited to the ProteomeXchange Consortium via the PRIDE partner repository<sup>27</sup> with the dataset identifier PXD015825

## **AUTHOR INFORMATION**

### **Corresponding Author**

\*e.tate@imperial.ac.uk

### **ORCID**

Nattawadee Panyain: 0000-0002-8279-6537

Aurélien Godinat: 0000-0002-6068-2512

Thomas Lanyon-Hogg: 0000-0002-7092-8096

Sofía Lachiondo-Ortega: 0000-0003-1856-3664

Edward J. Will: 0000-0003-4768-692X

Christelle Soudy: 0000-0003-2603-309X

Katie Mason: 0000-0001-7663-9781

Sarah Elkhalfa: 0000-0002-2827-202X

Lisa M. Smith: 0000-0002-2581-8760

Jeanine A. Harrigan: 0000-0001-8405-736X

Edward W. Tate: 0000-0003-2213-5814

### **Present Addresses**

<sup>||</sup>Liver Disease Laboratory, CIC bioGUNE, Bizkaia Technology Park, Derio, 48160, Spain

### **Author Contributions**

N.P. and A.G. undertook experiments, analyzed data and wrote the initial draft of the manuscript. T.L.-H. contributed to enzyme expression, assay data analysis and supervised experiments. S.L.-O. contributed to enzyme expression and assay data. E.W. and C.S. contributed to synthesis of compounds. K.M. performed biochemical screening assays, S.E. performed cellular activity probe assays, L.M.S. analyzed data and supervised experiments, and J.A.H generated UCHL1 expression constructs and supervised experiments. E.W.T. conceived and supervised the study. All authors contributed to the final version of the manuscript.

### **Notes**

K.M., S.E., L.M.S., and J.A.H. are employees of Mission Therapeutics Ltd; E.W.T. is a Director and shareholder in Myricx Pharma Ltd.

### **ACKNOWLEDGMENT**

The authors thank L. Haigh (Department of Chemistry Mass Spectrometry Facility, Imperial College London) for assistance in acquiring nanoLC–MS/MS, LC-ESI and high-resolution mass spectrometry (HRMS) data, C. Das (Purdue university) for his contributions to UCHL1 DNA construct, M. Morgan (Imperial College London) for assistance on structural studies, D. Conole (Imperial College London) for insightful comments on the manuscript, Charles River (Leiden, Netherlands) for FMT data, R. Williams, N. Jama and C. Stead (Mission Therapeutics) for technical assistance. This study was supported by Cancer Research UK (Programme Foundation Award C29637/A20183 to E.W.T.), Royal Thai Government scholarship (PhD studentship to N.P.), Swiss National Science Foundation (Early Postdoc Mobility Fellowship P2ELP2\_175069 to A.G.) and the Francis Crick Institute, which receives its core funding from Cancer Research UK (FC001097, FC010636), the UK Medical Research Council (FC001097, FC010636), and the Wellcome Trust (FC001097, FC010636).

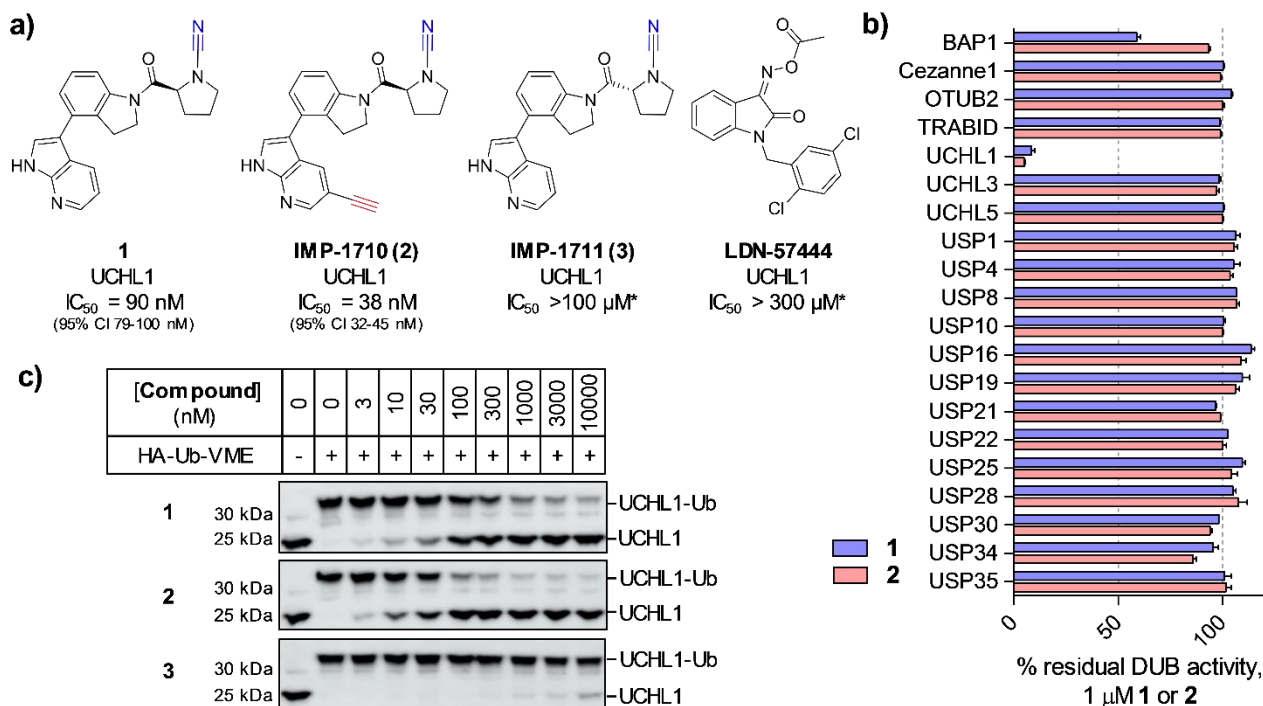


**Figure 1.** Specificity of UCHL1 inhibitor (**1**), alkyne ABP (IMP-1710, **2**), control compound (IMP-1711, **3**) and LDN-57444. (a) Inhibitor structures and UCHL1  $IC_{50}$  values (Ub-Lys-TAMRA FP assay). \*Maximum assay concentration. (b) Selectivity profiling of **1** and **2** against DUBs in FP and FI assays (Ub-Lys-TAMRA and Ub-Rho110, respectively). See Supplementary Information for **3** and LDN-57444 profiling. Data represent mean  $\pm$  SEM ( $n=2$ ). (c) Immunoblot analysis of HA-Ub-VME UCHL1 labeling following HEK293T treatment with **1**, **2** or **3** for 1 h. Dose-dependent decrease in UCHL1 labeling occurs with increasing active compounds, but not with inactive enantiomer **3**.



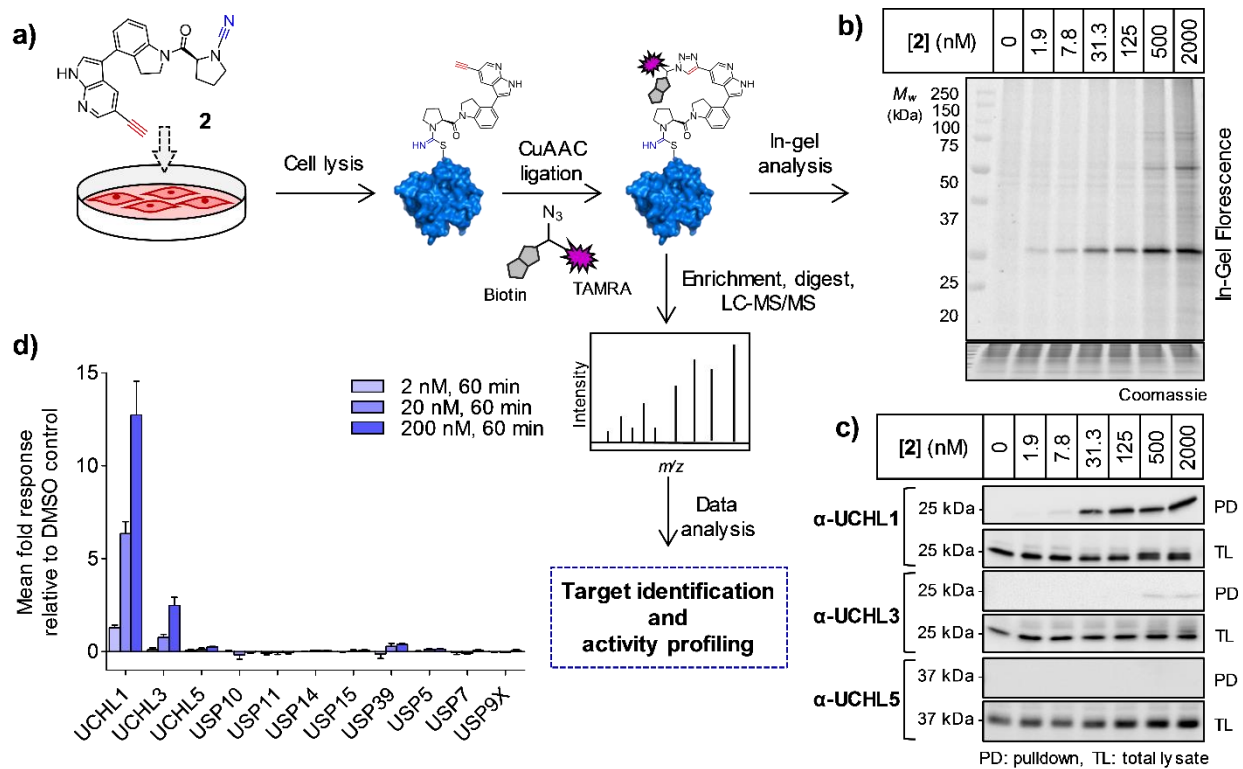


**Figure 2.** UCHL1 activity profiling using ABP **2** in HEK293 cells. (a) Chemical proteomics workflow. Cells were incubated with ABP **2**, and labeled proteins ligated *via* CuAAC to AzTB for in-gel fluorescence and/or affinity enrichment for immunoblotting and proteomic profiling. (b) In-gel fluorescence shows dose-dependent labeling by ABP **2**. (c) Probe-labeled protein identification by enrichment and immunoblotting. (d) Quantitative proteomic analysis of selected DUBs by ABP **2**, demonstrating dose-dependent enrichment of UCHL1. Data represent mean  $\pm$  SEM (n=3).

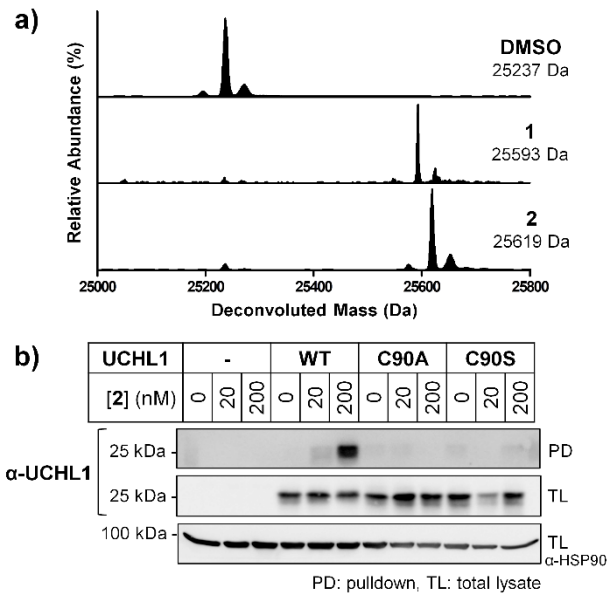


**Figure 3.** UCHL1 labeling with **1** and **2** exclusively at catalytic Cys90 *in vitro* and in intact cells. (a) LC-ESI demonstrating single UCHL1 covalent modification with **1** or **2**. (b) HeLa cells lacking endogenous UCHL1, transfected to express UCHL1 wild type (WT) or catalytic cysteine mutants (C90A and C90S); pull-down following treatment with **2** and AzTB functionalization confirms Cys90 specific labeling.

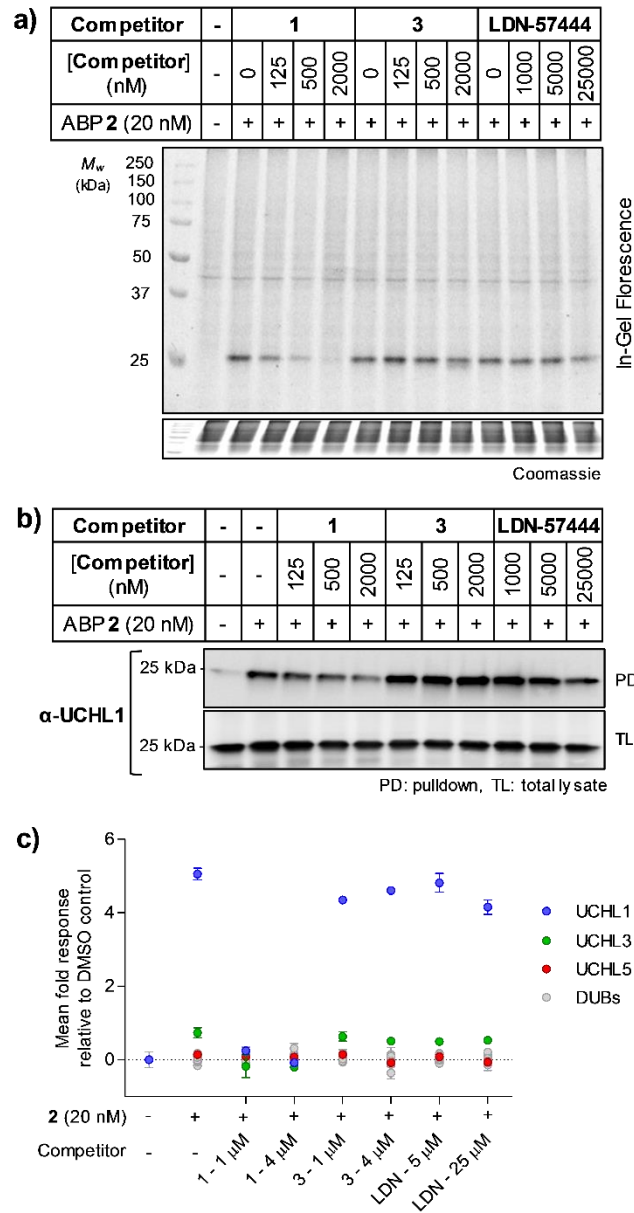


**Figure 4.** Compound **1** selectively competes ABP **2**, whilst **3** and LDN-57444 do not. Competition for ABP **2** labeling was confirmed by: (a) in-gel fluorescence; (b) pull-down and UCHL1 immunoblotting; (c) pull-down and whole proteome quantitative proteomic analysis. Data represent mean  $\pm$  SEM (n=3).

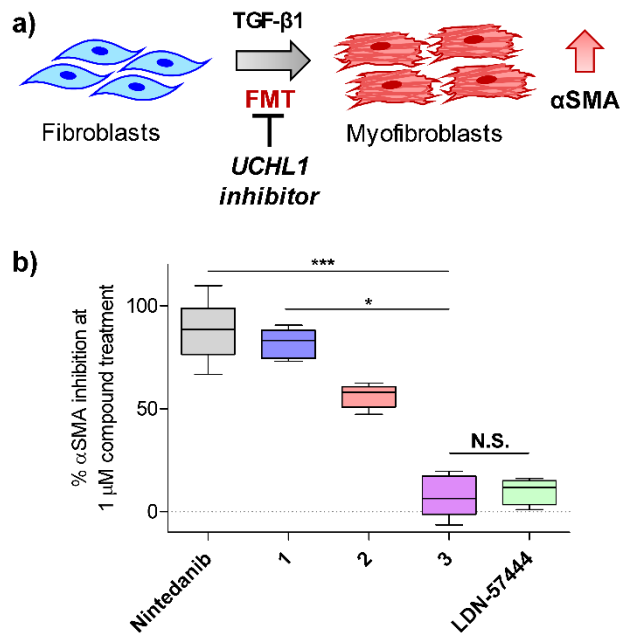
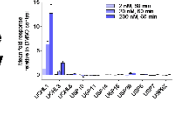
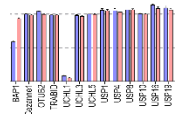
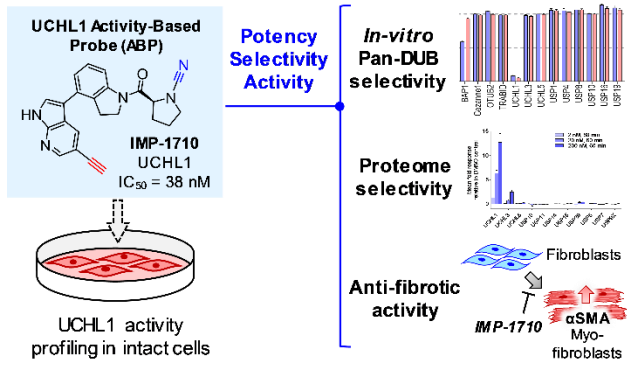


**Figure 5.** Phenotypic effects of selective UCHL1 inhibition in idiopathic pulmonary fibrosis (IPF). (a) Schematic of TGF- $\beta$ 1-mediated fibroblast-to-myofibroblast transition in primary human lung fibroblasts, increasing alpha-smooth muscle actin ( $\alpha$ SMA) transdifferentiation marker. (b) Primary fibroblasts from IPF donors were pre-incubated with 1  $\mu$ M **1**, **2**, **3**, LDN-57444, or IPF approved drug (nintedanib) for 1 h followed by TGF- $\beta$ 1 treatment for 3 days.  $\alpha$ SMA expression was analyzed by high content imaging, demonstrating **1**, **2**, and Nintedanib, but not **3** or LDN-57444 inhibit transdifferentiation (N.S. (non-significant), \* $P \leq 0.05$ , \*\*\* $P \leq 0.01$ ). Plots represent median values (center lines) and 25<sup>th</sup>/75<sup>th</sup> percentiles (box limits) with Tukey whiskers.

# Table of Contents (TOC)



## REFERENCES

1. Harrigan, J. A.; Jacq, X.; Martin, N. M.; Jackson, S. P., Deubiquitylating enzymes and drug discovery: emerging opportunities. *Nat Rev Drug Discov* **2018**, *17* (1), 57-78.
2. Hewings, D. S.; Flygare, J. A.; Bogoyo, M.; Wertz, I. E., Activity-based probes for the ubiquitin conjugation-deconjugation machinery: new chemistries, new tools, and new insights. *FEBS J* **2017**, *284* (10), 1555-1576.
3. Ward, J. A.; McLellan, L.; Stockley, M.; Gibson, K. R.; Whitlock, G. A.; Knights, C.; Harrigan, J. A.; Jacq, X.; Tate, E. W., Quantitative Chemical Proteomic Profiling of Ubiquitin Specific Proteases in Intact Cancer Cells. *ACS Chem Biol* **2016**, *11* (12), 3268-3272.
4. Bishop, P.; Rocca, D.; Henley, J. M., Ubiquitin C-terminal hydrolase L1 (UCH-L1): structure, distribution and roles in brain function and dysfunction. *Biochem J* **2016**, *473* (16), 2453-62.
5. Hurst-Kennedy, J.; Chin, L. S.; Li, L., Ubiquitin C-terminal hydrolase 1 in tumorigenesis. *Biochem Res Int* **2012**, *2012*, 123706.
6. Goto, Y.; Zeng, L.; Yeom, C. J.; Zhu, Y.; Morinibu, A.; Shinomiya, K.; Kobayashi, M.; Hirota, K.; Itasaka, S.; Yoshimura, M.; Tanimoto, K.; Torii, M.; Sowa, T.; Menju, T.; Sonobe, M.; Takeya, H.; Toi, M.; Date, H.; Hammond, E. M.; Hiraoka, M.; Harada, H., UCHL1 provides diagnostic and antimetastatic strategies due to its deubiquitinating effect on HIF-1 $\alpha$ . *Nat Commun* **2015**, *6*, 6153.
7. Wilson, C. L.; Murphy, L. B.; Leslie, J.; Kendrick, S.; French, J.; Fox, C. R.; Sheerin, N. S.; Fisher, A.; Robinson, J. H.; Tiniakos, D. G.; Gray, D. A.; Oakley, F.; Mann, D. A., Ubiquitin C-terminal hydrolase 1: A novel functional marker for liver myofibroblasts and a therapeutic target in chronic liver disease. *J Hepatol* **2015**, *63* (6), 1421-8.
8. Kemp, M.; Stockley, M.; Jones, A. Cyanopyrrolidines as Dub Inhibitors for the Treatment of Cancer. WO2017009650 (A1), 2017/01/19, 2017.
9. Broncel, M.; Serwa, R. A.; Ciepla, P.; Krause, E.; Dallman, M. J.; Magee, A. I.; Tate, E. W., Multifunctional reagents for quantitative proteome-wide analysis of protein modification in human cells and dynamic profiling of protein lipidation during vertebrate development. *Angew Chem Int Ed Engl* **2015**, *54* (20), 5948-51.
10. Storck, E. M.; Morales-Sanfrutos, J.; Serwa, R. A.; Panyain, N.; Lanyon-Hogg, T.; Tolmachova, T.; Ventimiglia, L. N.; Martin-Serrano, J.; Seabra, M. C.; Wojciak-Stothard, B.; Tate, E. W., Dual chemical probes enable quantitative system-wide analysis of protein prenylation and prenylation dynamics. *Nat Chem* **2019**, *11* (6), 552-561.
11. Geurink, P. P.; El Oualid, F.; Jonker, A.; Hameed, D. S.; Ovaa, H., A general chemical ligation approach towards isopeptide-linked ubiquitin and ubiquitin-like assay reagents. *Chembiochem* **2012**, *13* (2), 293-7.

12. Krabill, A. D.; Chen, H.; Hussain, S.; Feng, C.; Abdullah, A.; Das, C.; Aryal, U. K.; Post, C. B.; Wendt, M. K.; Galardy, P. J.; Flaherty, D. P., Biochemical and cellular characterization of a cyanopyrrolidine covalent Ubiquitin C-terminal hydrolase L1 inhibitor. *Chembiochem* **2019**.
13. Yabuki, N.; Watanabe, S.; Kudoh, T.; Nihira, S.; Miyamoto, C., Application of homogeneous time-resolved fluorescence (HTRFTM) to monitor poly-ubiquitination of wild-type p53. *Comb Chem High Throughput Screen* **1999**, *2* (5), 279-87.
14. Liu, Y.; Lashuel, H. A.; Choi, S.; Xing, X.; Case, A.; Ni, J.; Yeh, L. A.; Cuny, G. D.; Stein, R. L.; Lansbury, P. T., Jr., Discovery of inhibitors that elucidate the role of UCH-L1 activity in the H1299 lung cancer cell line. *Chem Biol* **2003**, *10* (9), 837-46.
15. Yan, C.; Huo, H.; Yang, C.; Zhang, T.; Chu, Y.; Liu, Y., Ubiquitin C-Terminal Hydrolase L1 regulates autophagy by inhibiting autophagosome formation through its deubiquitinating enzyme activity. *Biochem Biophys Res Commun* **2018**, *497* (2), 726-733.
16. Kobayashi, E.; Hwang, D.; Bheda-Malge, A.; Whitehurst, C. B.; Kabanov, A. V.; Kondo, S.; Aga, M.; Yoshizaki, T.; Pagano, J. S.; Sokolsky, M.; Shakelford, J., Inhibition of UCH-L1 Deubiquitinating Activity with Two Forms of LDN-57444 Has Anti-Invasive Effects in Metastatic Carcinoma Cells. *Int J Mol Sci* **2019**, *20* (15).
17. Larsen, C. N.; Price, J. S.; Wilkinson, K. D., Substrate binding and catalysis by ubiquitin C-terminal hydrolases: identification of two active site residues. *Biochemistry* **1996**, *35* (21), 6735-44.
18. Goya Grocin, A.; Serwa, R. A.; Morales Sanfrutos, J.; Ritzefeld, M.; Tate, E. W., Whole Proteome Profiling of N-Myristoyltransferase Activity and Inhibition Using Sortase A. *Mol Cell Proteomics* **2019**, *18* (1), 115-126.
19. Kalesh, K. A.; Clulow, J. A.; Tate, E. W., Target profiling of zerumbone using a novel cell-permeable clickable probe and quantitative chemical proteomics. *Chem Commun (Camb)* **2015**, *51* (25), 5497-500.
20. Clulow, J. A.; Storck, E. M.; Lanyon-Hogg, T.; Kalesh, K. A.; Jones, L. H.; Tate, E. W., Competition-based, quantitative chemical proteomics in breast cancer cells identifies new target profiles for sulforaphane. *Chem Commun (Camb)* **2017**, *53* (37), 5182-5185.
21. Cheng, J. C.; Tseng, C. P.; Liao, M. H.; Peng, C. Y.; Yu, J. S.; Chuang, P. H.; Huang, J. T.; Chen, J. J. W., Activation of hepatic stellate cells by the ubiquitin C-terminal hydrolase 1 protein secreted from hepatitis C virus-infected hepatocytes. *Sci Rep* **2017**, *7* (1), 4448.
22. Lepparanta, O.; Sens, C.; Salmenkivi, K.; Kinnula, V. L.; Keski-Oja, J.; Myllarniemi, M.; Koli, K., Regulation of TGF-beta storage and activation in the human idiopathic pulmonary fibrosis lung. *Cell Tissue Res* **2012**, *348* (3), 491-503.
23. Saito, A.; Horie, M.; Nagase, T., TGF-beta Signaling in Lung Health and Disease. *Int J Mol Sci* **2018**, *19* (8).

24. Grygielko, E. T.; Martin, W. M.; Tweed, C.; Thornton, P.; Harling, J.; Brooks, D. P.; Laping, N. J., Inhibition of gene markers of fibrosis with a novel inhibitor of transforming growth factor-beta type I receptor kinase in puromycin-induced nephritis. *J Pharmacol Exp Ther* **2005**, *313* (3), 943-51.
25. Richeldi, L.; du Bois, R. M.; Raghu, G.; Azuma, A.; Brown, K. K.; Costabel, U.; Cottin, V.; Flaherty, K. R.; Hansell, D. M.; Inoue, Y.; Kim, D. S.; Kolb, M.; Nicholson, A. G.; Noble, P. W.; Selman, M.; Taniguchi, H.; Brun, M.; Le Maulf, F.; Girard, M.; Stowasser, S.; Schlenker-Herceg, R.; Disse, B.; Collard, H. R.; Investigators, I. T., Efficacy and safety of nintedanib in idiopathic pulmonary fibrosis. *N Engl J Med* **2014**, *370* (22), 2071-82.
26. D'Arcy, P.; Wang, X.; Linder, S., Deubiquitinase inhibition as a cancer therapeutic strategy. *Pharmacol Ther* **2015**, *147*, 32-54.
27. Vizcaino, J. A.; Deutsch, E. W.; Wang, R.; Csordas, A.; Reisinger, F.; Rios, D.; Dienes, J. A.; Sun, Z.; Farrah, T.; Bandeira, N.; Binz, P. A.; Xenarios, I.; Eisenacher, M.; Mayer, G.; Gatto, L.; Campos, A.; Chalkley, R. J.; Kraus, H. J.; Albar, J. P.; Martinez-Bartolome, S.; Apweiler, R.; Omenn, G. S.; Martens, L.; Jones, A. R.; Hermjakob, H., ProteomeXchange provides globally coordinated proteomics data submission and dissemination. *Nat Biotechnol* **2014**, *32* (3), 223-6.